J Mater Sci (2011) 46:2155–2161
DOI 10.1007/s10853-010-5052-9

Microwave assisted synthesis of barium zirconium titanate nanopowders

V. Vinothini · B. Vaidhyanathan · J. Binner

Received: 1 June 2010 / Accepted: 3 November 2010 / Published online: 18 November 2010

Abstract The paper reports the synthesis, structural and high frequency dielectric properties of $\mathrm{Ba(Zr_{x}Ti_{1-x})O_{3,}}$BZT, nanopowders where $x = 0$, 0.1, 0.2, 0.3. These powders were synthesized using both microwave assisted and conventional heating, with the former requiring lower temperature and shorter times compared to the latter, viz., 700 °C for 30 min versus 900 °C for 5 h. The synthesized nanopowders were characterized using X-ray diffraction, micro-Raman spectroscopy, transmission electron microscopy, BET surface area analysis, differential scanning calorimetry and high frequency dielectric measurements. All the microwave synthesized BZT compositions were found to have well crystallized, finer nanoparticles with less agglomeration and higher dielectric permittivity compared to the conventionally prepared powders. The rapidity and less demanding processing conditions associated with the microwave assisted method augers well for the general applicability of the technique for the production of nanocrystalline powders.

Introduction

Recent trends in the electronics industry are towards the use of eco-friendly materials and processing techniques. Modified barium titanate (BT) ceramics are widely used as a replacement for Pb-based compositions, in line with regulatory requirements, for a variety of applications including multilayer capacitors, thermistors and optoelectronic devices [1]. At room temperature, $\mathrm{BaTiO_3}$ has a perovskite tetragonal crystal structure with large barium ions ($\mathrm{Ba^{2+}}$) on the corners of the unit cell, oxygen ($\mathrm{O^{2-}}$) in the face centres forming an octahedral arrangement and an off-centred, small titanium cation ($\mathrm{Ti^{4+}}$). Partial substitution of $\mathrm{Ti^{4+}}$ (ionic radius 0.745 nm) with $\mathrm{Zr^{4+}}$ (ionic radius 0.86 nm) forms the solid solution $\mathrm{Ba(Zr_{x}Ti_{1-x})O_3}$, BZT with an associated increase in the lattice parameter and consequent changes to the crystal structure, phase transition temperatures and the dielectric properties compared to pure BT [2]. Previous research performed using submicron-sized powders has suggested that BZT remains tetragonal at Zr additions of up to $\sim$0.2 mol%, then changes to pseudo-monoclinic over the range 0.2–0.6 mol% before becoming rhombohedral at Zr substitution levels up to $\sim$20 mol%. Above 20 mol% of Zr additions, BZT is cubic at room temperature [3]. Pure BT undergoes a sharp ferroelectric to paraelectric (tetragonal to cubic) transition at 130 °C. With up to 10 mol% of Zr, BZT ceramics exhibit a similar behaviour with a shift in the phase transition temperature from 130 to 110 °C. By 30 mol% of Zr addition, they show diffuse phase transition behaviour [4]. Above 30 mol%, the Zr-rich compositions exhibit diffuse phase transitions and dielectric dispersion, showing a relaxor-like behaviour [5]. Since these phase transition temperatures and phase boundary compositions will be dependent on the crystallite size of the primary particles, it is expected that the nanopowders might behave differently [6]. As the particle size is reduced to approximately that of the domain size of around tens of nanometres, the particles tend to stabilize to the nearest high symmetry crystal structure (cubic), presumably because of the high surface energy. This observation has been made in a range of different perovskite-structured oxides such as BT, BZT and $\mathrm{Pb(Zr_{0.52}Ti_{0.48})O_3}$ (PZT). The critical particle size at which this occurs is still unknown and seems to vary depending on the synthesis route used.

V. Vinothini · B. Vaidhyanathan (✉) · J. Binner
Department of Materials, Loughborough University,
Loughborough LE11 3TU, UK
e-mail: B.Vaidhyanathan@lboro.ac.uk

The ability to be able to make a nano BZT powder composition could result in improved reactivity, enhanced dielectric properties [7] and also enable device miniaturization [8]. Nano BZT powders have been prepared by a range of techniques, including sol–gel [9], co-precipitation [10] and hydrothermal [11] routes, amongst others. Although most of these approaches retain the stoichiometry and yield nanocrystalline powders, it is very difficult to avoid the formation of agglomerates [12]. If not eliminated during the green forming stage, the presence of these agglomerates results in the development of a bimodal grain size distribution during sintering, this significantly reduces the potential benefits arising from achieving nanostructured ceramics. In addition, all of the above techniques rely on a post-calcination stage to convert the as-prepared powder into the final, desired compound. As conventional heating relies on the conduction of heat through the insulating, powder-based precursor, it requires the use of long times at high temperatures, however, this leads to significant particle growth and turns otherwise soft agglomerates into hard agglomerates that are much more difficult to eliminate [13]. Hence, a rapid and efficient heating method would be useful. Microwaves can be used as an alternative energy source for processing during materials synthesis and sintering. The heat is generated by the interaction of the microwaves with the dielectric loss of the material; the internal nature of this interaction can enhance the reaction kinetics and hence reduce the processing temperature and/or time [14]. It should be noted, however, that to utilize the benefits of microwave processing, one of the reactants must have good microwave absorbing characteristics. The average power dissipated per unit volume of the material is given by

$$W = \frac{E_0^2 \omega \varepsilon_0 \varepsilon_r' \tan\delta}{2} \qquad (1)$$

where E_0—amplitude of the electric field ($E = E_0 \exp(j\omega t)$).

According to the equation, the power absorbed by the material depends on (i) the frequency and square of the amplitude of the electric field, and (ii) the dielectric constant and loss tangent of the material. The relative dielectric permittivity (ε_r') and loss tangent ($\tan\delta$) are the most important and measurable parameters. The ε_r' is a measure of polarizability of the materials in the electric field and $\tan\delta$ is a measure of the absorption of the microwave energy within the material [15–18].

In the present work, a simple, polymer-based precursor route was chosen for the synthesis of nano zirconium substituted BT since it results in homogeneously mixed ingredients and very fine, amorphous, carbon-containing intermediates with high dielectric loss values. This couples readily with the microwave field, leading to efficient and volumetric heating.

Experimental work

The intermediate precursor preparation followed in this study has been adapted from elsewhere [19] to suit the preparation of modified BT compositions. A titanium/zirconium solution was prepared by dissolving titanium tetraisopropoxide (98%, Aldrich, Steinheim, Germany) and zirconium nitrate (99%, MEL Chemicals, Manchester, UK) in a solution of citric acid (CA) (99.5%, Acros organics, New Jersey, USA) and ethylene glycol (EG) (98%, Fluka, Steinheim, Germany) keeping the CA:EG in a molar ratio of 1:4. The required quantity of $BaCO_3$ (99%, Fluka, Steinheim, Germany) was subsequently dissolved in the solution to yield a Ba: (Ti + Zr) ratio of 1:1. The zirconium content was varied from 0 to 30 mol% to form $BaTiO_3$ (BT), $Ba(Zr_{0.1}Ti_{0.9})O_3$ (BZT-10), $Ba(Zr_{0.2}Ti_{0.8})O_3$ (BZT-20) and $Ba(Zr_{0.3}Ti_{0.7})O_3$ (BZT-30), respectively. The solution was heated to 200 °C for 5 h in an oven to promote polymerization and remove solvents, the heat treatment yielding a solid, dark brown, glassy resin. Charring the resin further at 400 °C for 2 h resulted in a black solid mass, which was ground into a powder using an agate mortar and pestle. This powder is subsequently referred to in this article as the 'precursor'.

The microwave calcinations were performed in a multimode cavity operating at 2.45 GHz and capable of providing an adjustable, continuous output power up to a maximum of 6 kW. However, the use of 1200 W was found enough to reach the required temperature. The precursors were placed in silica crucibles inside the microwave cavity with appropriate thermal insulation to reduce the heat loss (Fig. 1). The calcination temperature was varied from 550 to 700 °C in 50 °C intervals and for 30 or 60 min at each temperature. An optical pyrometer (Minolta/Land Cyclops 152, Land Infrared, Sheffield, UK) was used to measure the temperature of the material during microwave heating and a thermal imaging camera (FLIR

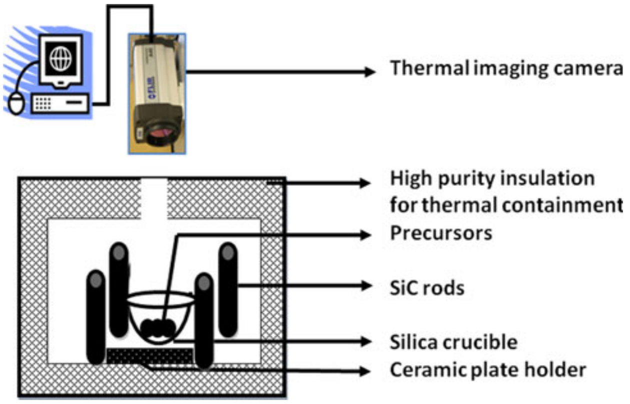

Fig. 1 Sample arrangements in the microwave cavity for nano BZT synthesis

Systems, ThermoVisionTM® A40, Boston, USA) was used to measure the temperature distribution across the sample as described elsewhere [20–22]. The temperature calibration was performed using the melting point of Vanadium pentoxide and the accuracy of temperature measurements was found to be within ±5 °C. For comparison, the precursors were also calcined using conventional heating from 600 to 900 °C for a period of 5 h. A K-type thermocouple was used to measure the temperature of the sample; no attempt was made to measure the temperature distribution across the sample in this case, rather it was assumed to be homogeneous given the duration of the calcinations.

The phases formed in each of the synthesized powder batches was analyzed using powder X-ray diffractometry (XRD) using Cu Kα radiation (Bruker D8 model diffractometer, Bruker AXS GmbH, Karlsruhe, Germany) and micron-Raman spectroscopy (Horiba Yvon Raman LabramHR spectrometer, Horiba Jobin Yvon SAS, Villeneuve d'Ascq, France). The powder particle size was assessed using transmission electron microscopy (JEOL JEM 2000FX, JEOL Ltd. Tokyo, Japan) and the dielectric properties were measured at 2.47 GHz using a cavity perturbation method [23] at the Nottingham University, UK. These measurements were used to obtain the dielectric loss characteristics of both the precursors and the products. The temperature dependant dielectric property data also yielded the Curie transition temperatures of the BZT powders, which were further corroborated using differential scanning calorimetry measurements (MDSC, TA instruments, Q2000, New Castle, USA).

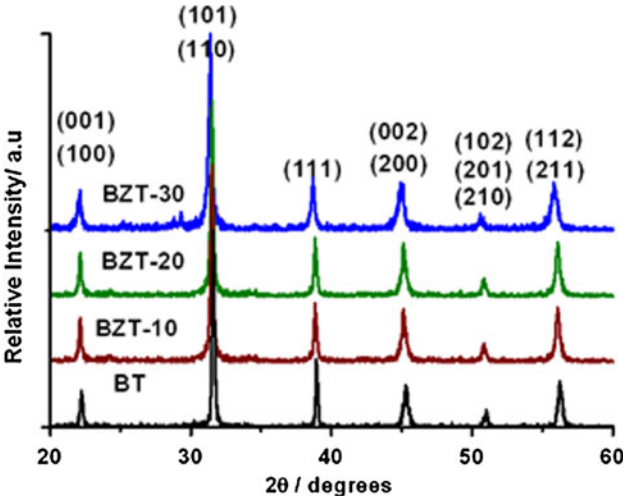

Fig. 2 XRD patterns of the BT, BZT-10 and BZT-20 precursors calcined at 900 °C for 5 h using conventional heating

Results and discussion

The dielectric properties of the starting precursors ($\tan \delta = 0.02$; $\varepsilon'' = 0.05$) show that the precursors have reasonably high values of relative permittivity and loss tangent (comparative $\tan \delta$ value for microwave transparent quartz is 0.0001 and $\varepsilon'' = 0.0004$) [24].

The XRD patterns of the precursors calcined by conventional heating at 900 °C for 5 h are shown in Fig. 2. All the compositions up to 20 mol% Zr substitutions formed the single phase tetragonal structure above which it formed the cubic structure (Table 1); at lower temperatures the reactions were not complete and varying quantities of the reactants were detected.

Figure 3 shows clearly how the diffraction peaks shifted to lower angles with increasing Zr content, suggesting an increase in unit cell volume. The Raman spectra for the BZT compositions calcined at 900 °C for 5 h using conventional heating, Fig. 4, also show that the sample retained the tetragonal crystal structure up to 20 mol% of Zr substitution and on further Zr addition it started losing tetragonality and changed to cubic symmetry. The intensity of the main tetragonal peak at 307 cm^{-1} was found to decrease with increasing Zr addition. However, there was no indication of the pseudo-monoclinic or rhombohedral phases observed by other researchers [25, 26]. With increasing Zr, an additional peak at 123 cm^{-1} was observed as expected; this mode corresponded to the vibration of Zr atoms in the lattice, which was in agreement with previous results [25]. Similarly, the vibration of Ti atoms in the oxygen octahedra caused the peak at 180 cm^{-1}, which decreased in intensity as the ratio of Zr/Ti increased.

Table 1 Lattice parameters of BT, BZT-10, BZT-20 and BZT-30 precursors calcined at 900 °C for 5 h in conventional heating and 700 °C for 30 min in microwave heating (c/a ±0.0004)

CON	*a* (nm)	*c* (nm)	*c*/*a*	Lattice volume (nm^3)	MW	*a* (nm)	*c* (nm)	*c*/*a*	Lattice volume (nm^3)
BT	4.000	4.017	1.004	64.27	BT	4.008	4.026	1.005	64.67
BZT-10	4.006	4.025	1.004	64.59	BZT-10	4.009	4.027	1.005	64.72
BZT-20	4.013	4.023	1.003	64.79	BZT-20	4.013	4.026	1.003	64.84
BZT-30	4.03	4.03	1.000	65.40	BZT-30	4.026	4.041	1.003	65.48

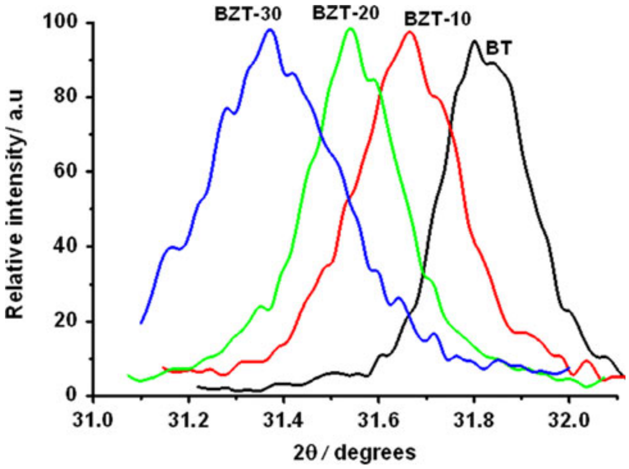

Fig. 3 Magnified view of the shift of the (110) X-ray diffraction peak of the BT, BZT-10, BZT-20 and BZT-30 precursors calcined at 900 °C for 5 h using conventional heating

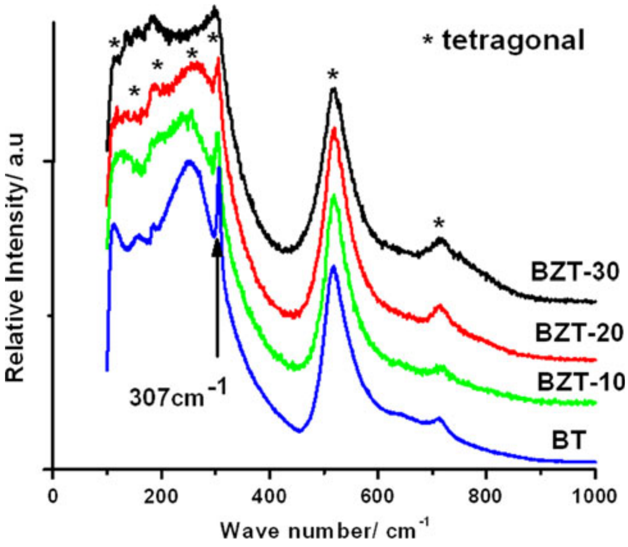

Fig. 4 Raman spectra of BT, BZT-10, BZT-20 and BZT-30 precursors calcined at 900 °C for 5 h in conventional heating

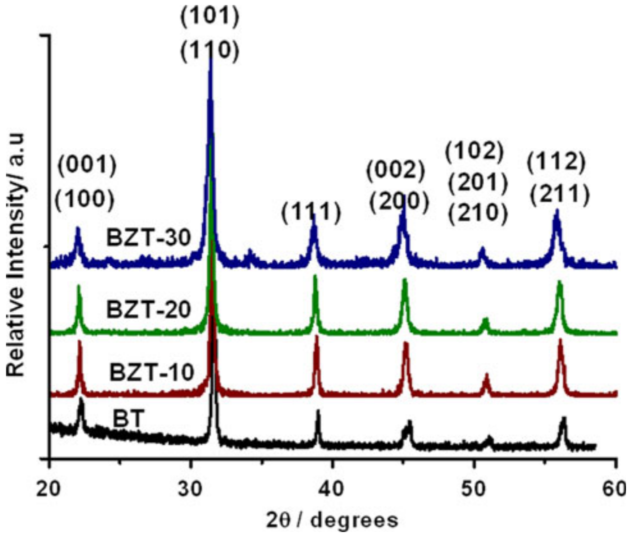

Fig. 5 XRD pattern of BT, BZT-10, BZT-20 and BZT-30 precursors calcined at 700 °C for 30 min in microwave heating

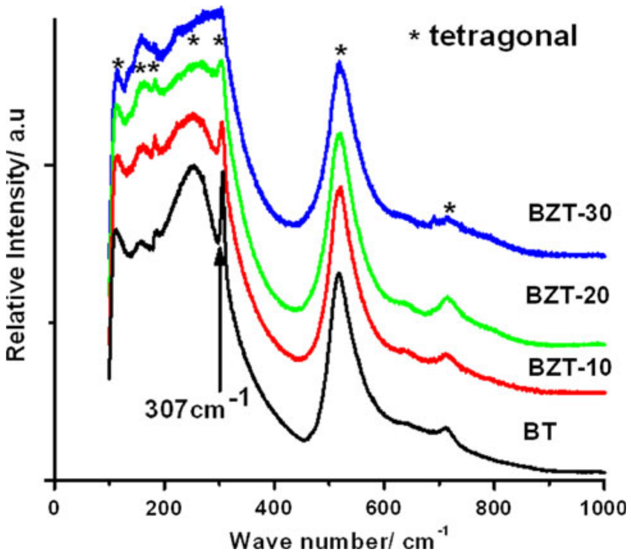

Fig. 6 Raman spectra of BT, BZT-10, BZT-20 and BZT-30 precursors calcined at 700 °C for 30 min using microwave heating

Figure 5 shows the XRD pattern of the BZT precursors calcined at 700 °C for 30 min using microwave heating. All the peaks were found to be characteristic of the tetragonal structure. The Raman spectra for the microwave calcined BZT powders, Fig. 6, confirmed the high tetragonality (exhibiting the signature peak at 307 cm^{-1}) of the powders produced. Similar peaks were obtained as found for conventional calcined powders were obtained. The calculated lattice parameters for the conventional and microwave calcined nanopowders are shown in Table 1. With the increase in Zr substitution, the cell parameters increase as the ionic radii of Zr is larger than that for Ti, hence the cell volume increases. Microwave calcined powders exhibit slightly larger cell volumes whilst maintaining high tetragonality. Similar observations were made during the microwave assisted sintering of Sr substituted $BaTiO_3$ [27]. The lattice strain associated with the higher cooling rates in the microwave process could also be a contributing factor. Microwave assisted improvement on tetragonality of the nano BT powders was also reported by Sun and Li [28].

The particle sizes of the powders synthesized using the conventional and microwave heating are shown in Fig. 7. The microwave calcined powders had a uniform and finer particle size of ~30 nm with less evidence of agglomeration compared to the conventionally calcined powders, which had mean particle sizes in the range of 50–100 nm. It is believed that this result is due to the rapid heating and

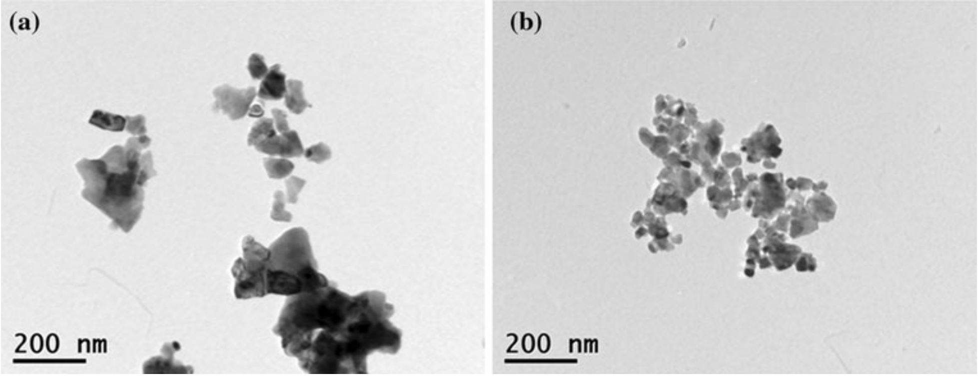

Fig. 7 TEM images of the BZT-20 powders calcined at **a** 900 °C for 5 h using conventional heating and **b** 700 °C for 30 min using microwave heating

Table 2 BET surface area results of the BZT compositions calcined using different heating methods

Compositions	Conventional heating (m^2/g)	Microwave heating (m^2/g)
BT	2.7	6.1
BZT-10	5.5	6.7
BZT-20	12.2	14.0
BZT-30	5.7	7.8

cooling associated with microwave heating that provides less time for particle growth and agglomeration [27]. Table 2 provides the surface areas of the microwave and conventionally heated powders and the smaller particle size and lower extent of agglomeration of the microwave powders were probably instrumental in explaining the higher surface areas observed. The lower temperature employed in the microwave process was also probably responsible for the finer crystallite size and larger surface area of the microwave prepared powders obtained.

The finer particles sizes, higher surface area and the associated better tetragonality of the microwave prepared nanopowders also had an influence on the high frequency dielectric properties observed, Table 3. All the compositions of the microwave calcined powders were found to have higher relative permittivity values. The BZT-10 showed a phase transition at 82 °C, Fig. 8, which compares well with the literature [29]. It has been reported that in BT, the enthalpy of phase transition decreases with decreasing particle size [30]. For the materials synthesized here, the ΔH of the microwave calcined BT powder (0.1 J/mol K) is found to be lower than that of the conventionally calcined BT powder (0.35 J/mol K); this could be because of the finer particle size and reduced degree of agglomeration noticed in the microwave calcined BT powders.

Table 3 Dielectric properties of the BZT compositions calcined using conventional and microwave heating

CON	ε'	ε''	MW	ε'	ε''
BT	3.5	0.1	BT	4.95	0.1
BZT-10	7.18	0.2	BZT-10	13.57	0.2
BZT-20	6.11	0.2	BZT-20	12.11	0.3
BZT-30	4.79	0.08	BZT-30	6.73	0.05

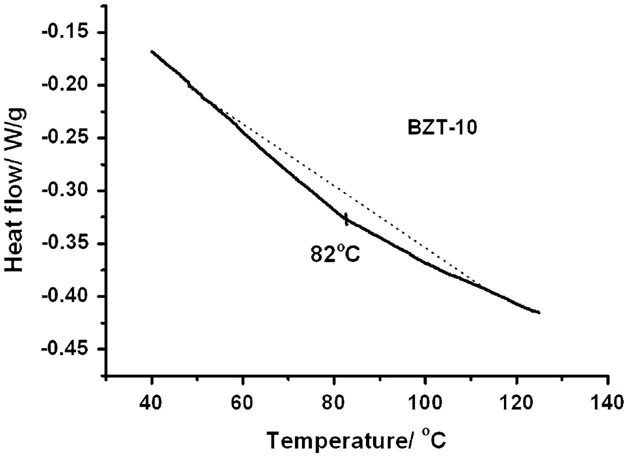

Fig. 8 Typical DSC of the BZT-10 composition

It is interesting to note that when microwaves were used, full tetragonality could be obtained at temperatures 200 °C lower and with 1/10th of the soaking time required for conventional methods. There is now a significant database of evidence in the literature that suggests that microwaves have the ability to accelerate or enhance reaction and diffusion rates during materials processing. A number of mechanisms have been suggested to account for this behaviour [31–35]. Some of the previous work suggested that the diffusion of Ba^{2+} and Ti^{4+} were enhanced in the microwave field, hence influencing the diffusion coefficient and the driving force for ion motion [36]. Similar results were also reported during the synthesis of lead zirconium titanate [37]. Comparing the time–temperature profiles for the microwave and conventional BZT calcinations, Fig. 9

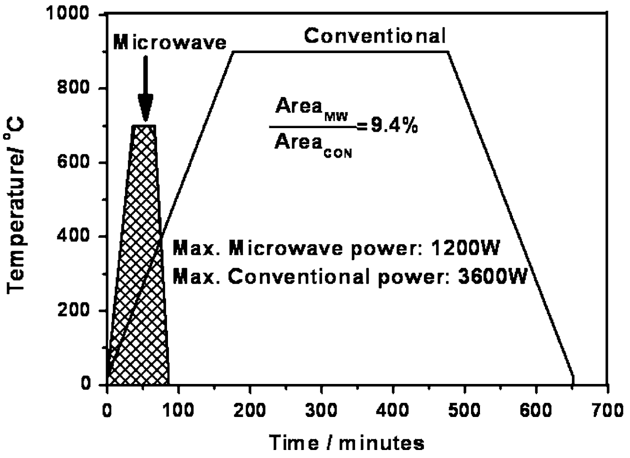

Fig. 9 Time–temperature profiles of the conventional and microwave calcinations cycles

indicate the extent of reduction in processing time and temperature. The simple calculation of the area under the curve, which is a very rough estimate of the energy involved in the process, indicates that microwave processing requires only ~10% of the energy required when compared to the conventional method whilst operating at a 66% lower power level. Even to achieve the same temperature, say 900 °C, the amount of microwave power required was found to be 1400 W whilst for the conventional furnace it was 3600 W. The enhancement in reaction kinetics in microwave assisted reactions could be due to the volumetric nature of the heating and hence the bulk nucleation [38], effective use of reaction enthalpies [39] and the employment of an additional driving force for diffusion resulting from the E-field component of the microwave radiation [40].

Conclusions

Single phase crystalline BZT nano powders with less agglomeration were synthesized using microwave assisted heating under less demanding processing conditions (700 °C/30 min) compared to conventional heating (900 °C/5 h). The crystallinity and the dielectric permittivity of the microwave synthesized BZT nanopowders were assessed to be better than the conventionally calcined powders. The microwave technique is also found to be generically applicable for the rapid preparation of nanocrystalline BSZT ($Ba_{1-x}Sr_xZr_{0.1}Ti_{0.9}O_3$) formulations. The lower temperatures and shorter processing times used as well as the high surface area, fine grained nanopowders obtained makes it an attractive synthesis methodology.

Acknowledgements The authors thank the EPSRC/TSB of the United Kingdom for the research funding and one of the authors (VV) thank the Science Faculty Fellowship Fund of the Loughborough University for her PhD scholarship. Thanks are also due to Dr. George A Dimitrakis of the Nottingham University, UK for timely help with the high frequency dielectric measurements.

References

1. Jaffe B, Cook WR, Jaffe H (1981) Piezoelectric ceramics. Academic Press, New York, p 271
2. Bernadi MLB, Antoneli E, Lourenco AB, Feitosa CAC, Maia LJQ, Hernades AC (2007) J Therm Anal Calorim 87:725
3. Landolt-Bornstein (1981) Landolt-Bornstein numerical data and functional relationship in science and technology. Springer-Verlag, Berlin, vol III/28a, p 268; vol III/16a, p 422
4. Hennings D, Schnell A (1982) J Am Ceram Soc 65:539
5. Neirman SM (1988) J Mater Sci 23:3973. doi:10.1007/BF01106823
6. McCauley D, Newnham RE, Randall CA (1998) J Am Ceram Soc 81:979
7. Chen JF, Shen ZG, Liu FT, Liu XL, Yun J (2003) Scripta Mater 49:509
8. Tang XG, Wang J, Wang XX, Chan HLW (2004) Solid State Commun 131:163
9. Kumar M, Garg A, Kumar R, Bhatnagar MC (2008) Phys B 403:1819
10. Reddy SB, Rao KP, Rao MSR (2007) Scripta Mater 57:591
11. Outzourhit A, Idrissi Raghni MAE, Hafid ML, Bensamka F, Abdelkader O (2002) J Alloys Compd 340:214
12. Gogotsi Y (2006) Nanomaterials handbook. Taylor & Francis, London, p 363
13. Binner J, Vaidhyanathan B (2008) J Eur Ceram Soc 28:1329
14. Rao KJ, Vaidhyanathan B, Ganguli M, Ramakrishnan PA (1999) Chem Mater 11:882
15. Janney MA, Kimrey HD (1991) Microwave processing of materials II. In: Snyder WB Jr, Sutton WH, Iskander MF, Johnson DL (eds) Materials Research Society Symposium Proceedings, vol 189, p 215
16. Sutton WH (1992) Microwave processing of materials III. In: Beatty RL, Sutton WH, Iskander MF (eds) Materials Research Society Symposium Proceedings, vol 269, p 3
17. Clark DE (1997) Microwaves: theory and application in materials processing IV. In: Clark D, Sutton WH, Lewis DA (eds) Ceramics Transactions, vol 80, p 61
18. Robb GR, Harrison A, Whittaker AG (2002) Phys Chem Commun 19:135
19. Vinothini V, Singh P, Balasubramanian M (2006) Ceram Int 32:99
20. Vaidhyanathan B, Wang J, Binner JGP, Raghavendra R (2003) The effect of conventional, microwave and hybrid heating on the sintering of ceramics. In: 9th international conference on microwave and high frequency heating, Loughborough, p 31
21. Vaidhyanathan B, Annapoorani K, Binner JGP, Raghavendra R (2009) Ceram Eng Sci Proc 30:11
22. Wang J, Binner J, Vaidhyanathan B (2006) J Am Ceram Soc 89:1977
23. Dimitrakis GA (2005) PhD Thesis, University of Nottingham
24. Plonskii YA, Pavlova GA, Savel'ev VN, Milovidova TV, Vinogradov VB (1971) Glass Ceram 28:182
25. Dobal PS, Dixit A, Katiyar RS, Yu Z, Guo R, Bhalla AS (2001) J Raman Spectrosc 32:69
26. Qi JQ, Wang Y, Chen WP, Li LT, Chan HTW (2006) J Nanoparticle Res 8:959

27. Thakur OP, Prakash C, Agarwal DK (2002) Mater Sci Eng B96:221
28. Sun W, Li J (2006) Mater Lett 60:1599
29. Ho IC, Fu SL (1990) J Mater Sci 25:4699. doi:10.1007/BF01129927
30. Asiaie R, Zhu W, Akbar SA, Dutta PK (1996) Chem Mater 8:226
31. Fathi Z, Ahmed I, Simmons JH, Clark DE, Lodding AR (1991) Microwaves: theory and application in materials processing. In: Clark DE, Gac FD, Sutton WH (eds) Ceram Transactions, vol 21, p 623
32. Hassine JGP, Hassine NA, Cross TE (1995) J Mater Sci 30:5389. doi:10.1007/BF00351548
33. Rybakov KI, Semenov VE (1994) Phys Rev B 49:64
34. Rybakov KI, Semenov VE (1995) Phys Rev B 52:3032
35. Hanxing L, Yongwei L, Hanlin Z, Shixi O (1997) Sci China Ser A 40:843
36. Zhang H, Ouyang S, Liu H, Li Y (1996) Microwave processing of materials V. In: Iskander MK, Kiggans JO, Bolomey JC (eds) Materials Research Society Symposium Proceedings, vol 430, p 447
37. Vaidhyanathan B, Singh AP, Agrawal DK, Shrout TR, Roy R (2001) J Am Ceram Soc 84:1197
38. Vaidhyanathan B, Binner JGP (2006) J Mater Sci 41:5954. doi:10.1007/s10853-006-0260-z
39. Vaidhyanathan B, Raizada P, Rao KJ (1997) J Mater Sci Lett 16:2022
40. Willert-Porada M, Bartusch W, Dhupia G, Müller G, Nagel A, Wötting G (2000) In: Müller G (ed) Ceramics-processing, reliability, tribology and wear. Euromat 12:87. Wiley-VCH, Berlin